Combined crossed beam and theoretical studies of the C(D−1) + CH4 reaction

ARTICLE *in* THE JOURNAL OF CHEMICAL PHYSICS · JANUARY 2013

Impact Factor: 2.95 · DOI: 10.1063/1.4773579 · Source: PubMed

6 AUTHORS, INCLUDING:

Dimitrios Skouteris
Scuola Normale Superiore di Pisa
68 PUBLICATIONS **1,171** CITATIONS
SEE PROFILE

Piergiorgio Casavecchia
Università degli Studi di Perugia
168 PUBLICATIONS **4,272** CITATIONS
SEE PROFILE

Marzio Rosi
Università degli Studi di Perugia
191 PUBLICATIONS **2,643** CITATIONS
SEE PROFILE

Nadia Balucani
Università degli Studi di Perugia
162 PUBLICATIONS **3,433** CITATIONS
SEE PROFILE

Combined crossed beam and theoretical studies of the C(1D) + CH4 reaction

Francesca Leonori, Dimitrios Skouteris, Raffaele Petrucci, Piergiorgio Casavecchia, Marzio Rosi et al.

Citation: J. Chem. Phys. **138**, 024311 (2013); doi: 10.1063/1.4773579
View online: http://dx.doi.org/10.1063/1.4773579
View Table of Contents: http://jcp.aip.org/resource/1/JCPSA6/v138/i2
Published by the American Institute of Physics.

Combined crossed beam and theoretical studies of the $C(^1D) + CH_4$ reaction

Francesca Leonori,[1] Dimitrios Skouteris,[1] Raffaele Petrucci,[1] Piergiorgio Casavecchia,[1] Marzio Rosi,[2] and Nadia Balucani[1,a)]

[1]*Dipartimento di Chimica, Università degli Studi di Perugia, 06123 Perugia, Italy*
[2]*Dipartimento di Ingegneria Civile e Ambientale and ISTM-CNR, Università degli Studi di Perugia, 06123 Perugia, Italy*

(Received 8 November 2012; accepted 12 December 2012; published online 10 January 2013)

The reaction involving atomic carbon in its first electronically excited state ^1D and methane has been investigated in crossed molecular beam experiments at a collision energy of 25.3 kJ mol^{-1}. Electronic structure calculations of the underlying potential energy surface (PES) and Rice–Ramsperger–Kassel–Marcus (RRKM) estimates of rates and branching ratios have been performed to assist the interpretation of the experimental results. The reaction proceeds via insertion of $C(^1D)$ into one of the C–H bonds of methane leading to the formation of the intermediate $HCCH_3$ (methylcarbene or ethylidene), which either decomposes directly into the products $C_2H_3 + H$ or $C_2H_2 + H_2$ or isomerizes to the more stable ethylene, which in turn dissociates into $C_2H_3 + H$ or $H_2CC + H_2$. The experimental results indicate that the H-displacement and H_2-elimination channels are of equal importance and that for both channels the reaction mechanism is controlled by the presence of a bound intermediate, the lifetime of which is comparable to its rotational period. On the contrary, RRKM estimates predict a very short lifetime for the insertion intermediate and the dominance of the H-displacement channel. It is concluded that the reaction $C(^1D) + CH_4$ cannot be described statistically and a dynamical treatment is necessary to understand its mechanism. Possibly, nonadiabatic effects are responsible for the discrepancies, as triplet and singlet PES of methylcarbene cross each other and intersystem crossing is possible. Similarities with the photodissociation of ethylene and with the related reactions $N(^2D) + CH_4$, $O(^1D) + CH_4$ and $S(^1D) + CH_4$ are also commented on. © *2013 American Institute of Physics*. [http://dx.doi.org/10.1063/1.4773579]

I. INTRODUCTION

The lowest electronically excited state of atomic carbon, ^1D, is metastable with a lifetime of 3230 s and an energy content of 121.8 kJ mol^{-1} with respect to the ground ^3P state.[1,2] The reactivity of $C(^1D)$ with several molecules having strong σ bonds (e.g., H_2, CH_4) is much larger than that of $C(^3P)$,[1] because $C(^1D)$ insertion into H–H and C–H bonds is barrierless. The reactions $C(^1D) + H_2$ and $C(^1D) + CH_4$ are indeed fast (close to the gas kinetics limit),[1] whereas the corresponding reactions involving $C(^3P)$ are much slower (the reaction $C(^3P) + H_2$ is endothermic[3] while the reaction $C(^3P) + CH_4$ is characterized by an entrance barrier of 51 kJ mol^{-1}).[4] In particular, the reaction $C(^1D) + H_2$ (which is among the best characterized tri-atomic reactions, see Refs. 5–8, and references therein) is a barrierless reaction where the insertion of $C(^1D)$ into the H–H bond generates the strongly bound intermediate $CH_2(\tilde{a}\ ^1A_1)$ which, in turn, dissociates into the products $CH(X\ ^2\Pi) + H$. The effect of singlet excited state potential energy surfaces (PES) has been recently considered for this reaction, as the interaction of the fivefold degenerate $C(^1D)$ atom with H_2 generates five singlet PESs, of which at least the first excited $1^1A''$ can make a contribution to the global reactivity.[8,9] In addition, the ground state singlet PES correlating with the singlet $\tilde{a}\ ^1A'$ state of CH_2 is characterized by the presence of two crossings with the triplet PES describing the $C(^3P) + H_2$ system, which is also characterized by the presence of a deep well corresponding to the ground state $X\ ^3B_1$ of the CH_2 radical.[3,10] The two CH_2 low-lying singlet and triplet states are known to be strongly mixed and the interaction between the triplet and singlet surfaces has been called into play to explain the large difference between theoretical and experimental rate constants for the related reverse reaction $CH(^2P) + H(^2S)$.[11]

In addition to $C(^1D) + H_2$, the only other $C(^1D)$ reactions for which reaction dynamics investigations are available so far are those involving several unsaturated hydrocarbons (C_2H_2, C_2H_4, and C_3H_6)[12–15] and HCl.[16] In the case of the reactions of $C(^1D)$ with unsaturated hydrocarbons, the favored approach is addition to the π bond, rather than insertion into one of the C–H bonds, while in the case of the reaction with HCl insertion is the dominant approach and, quite interestingly, the yield of CCl product is larger than that of CH.[16] In this paper, we report on the first study of the reaction mechanism for the system $C(^1D) + CH_4$.

The reaction of ground state carbon atoms with methane has been investigated in previous work. Electronic structure calculations of the triplet C_2H_4 PES and Rice–Ramsperger–Kassel–Marcus (RRKM) calculations have been performed

a)Author to whom correspondence should be addressed. Electronic mail: nadia.balucani@unipg.it.

by Kim *et al.*,[4] while a laser-induced-fluorescence (LIF) experiment has been carried out by Scholefield *et al.*[17] According to the calculations by Kim *et al.*,[4] the favored approach is insertion of $C(^3P)$ into a C–H bond of CH_4 with formation of the triplet intermediate $HCCH_3(^3A'')$. $HCCH_3$ can directly dissociate into $C_2H_3(^2A') + H$ or rearrange to triplet $C_2H_4(^3A')$ before fragmenting into the same products or into $C_2H_2(^3B_2) + H_2$ or $H_2CC(^3B_2) + H_2$. The possible products are, therefore,

$$C(^3P)+CH_4 \rightarrow C_2H_3(^2A')+H \quad \Delta H^\circ_{298} = -115.9\,\text{kJ mol}^{-1}, \tag{1a}$$

$$\rightarrow C_2H_2(^3B_2)+H_2 \quad \Delta H^\circ_{298} = -36.0\,\text{kJ mol}^{-1}, \tag{1b}$$

$$\rightarrow H_2CC(^3B_2)+H_2 \quad \Delta H^\circ_{298} = -25.1\,\text{kJ mol}^{-1}, \tag{1c}$$

$$\rightarrow CH(^2\Pi)+CH_3 \quad \Delta H^\circ_{298} = +99.6\,\text{kJ mol}^{-1}. \tag{1d}$$

(The reported enthalpies of reactions are those calculated by Kim *et al.*[4] using the CCSD(T)/6-311+G(3df,2p)//QCISD/6-311G(d,p) method). The calculations by Kim *et al.*[4] derived an entrance barrier of 51 kJ mol^{-1} for the favored insertion channel, while H-abstraction is characterized by a much larger entrance barrier of 112.5 kJ mol^{-1}. By using hyperthermal (>2 eV) carbon atoms, Scholefield *et al.*[17] were able to overcome the insertion entrance barrier and to determine the distribution of rotational states of the CH product generated in channel (1d). The experimental results are consistent with the formation of a bound intermediate, but RRKM calculations by Kim *et al.*[4] indicated that CH formation at those high collision energies should be dominated by direct H-abstraction. Quite interestingly, Kim *et al.*[4] have found that intersystem crossing (ISC) from the singlet to the triplet PES is possible in the vicinity of the insertion intermediate HC-CH_3 because of the small difference in energy of the triplet and singlet state of methylcarbene. The energy splitting (12.8 kJ mol^{-1} at the W1 level of the present calculations, see below) is much lower than that associated to $CH_2(X\ ^3B_1, \tilde{a}\ ^1A_1)$ ($\sim$37 kJ mol^{-1}).[18]

The reaction of $C(^1D)$ with methane is characterized by channels similar to those shown for the reaction $C(^3P) + CH_4$, but they are much more exothermic because of the excitation energy of atomic carbon and because acetylene and H_2CC are formed in their ground singlet states,

$$C(^1D) + CH_4 \rightarrow C_2H_3(^2A') + H \quad \Delta H^\circ_0 = -250.8\,\text{kJ mol}^{-1}, \tag{2a}$$

$$\rightarrow C_2H_2(^1\Sigma_g^+) + H_2 \quad \Delta H^\circ_0 = -536.7\,\text{kJ mol}^{-1}, \tag{2b}$$

$$\rightarrow H_2CC(^1A_1) + H_2 \quad \Delta H^\circ_0 = -353.8\,\text{kJ mol}^{-1}, \tag{2c}$$

$$\rightarrow CH(^2\Pi) + CH_3(^2A_2) \quad \Delta H^\circ_0 = -24.9\,\text{kJ mol}^{-1}, \tag{2d}$$

$$\rightarrow CCH_3(^2A'') + H \quad \Delta H^\circ_0 = -45.0\,\text{kJ mol}^{-1}. \tag{2e}$$

(The reported enthalpies of reactions are calculated in this work at the W1 level, see below.) The most exothermic channel is now the one leading to acetylene and molecular hydrogen (2b) followed by the one leading to the vinylidene radical and molecular hydrogen (2c). In this case also the channel leading to CH is exothermic (2d) and an additional channel leading to $CCH_3 + H$ is present. We have investigated reaction (2) by using the crossed molecular beam (CMB) technique with mass spectrometric (MS) detection. In addition, electronic structure calculations of the underlying ground state singlet PES and RRKM estimates of the product branching ratio have been performed to assist the interpretation of the scattering results.

The results of this study will be compared with ethylene vacuum ultraviolet (VUV) photodissociation,[19,20] because some regions of the same PES[21,22] are experienced by the two processes (insertion of $C(^1D)$ into one methane bond is a way to form activated ethylene or methylcarbene). Finally, the reaction mechanism will be compared with those of the related systems $O(^1D) + CH_4$, $N(^2D) + CH_4$ and $S(^1D) + CH_4$, which have been already investigated in CMB experiments.[23–25]

We would like to remark that the $C(^1D) + CH_4$ reactive system is not only interesting from a fundamental point of view. On the contrary, it can play a major role in the chemistry of the coma of comets approaching the Sun (both methane and $C(^1D)$ have been identified in cometary comae[26–28] and, when the outgas of the comet nucleus is strong because of the vicinity to the Sun, bimolecular collisions occur[28]) and in chemical vapor deposition of nanodiamonds, where electronically excited species can play a role.[29]

This paper is organized as follows. In Sec. II we describe the crossed-beam experiments. In Sec. III computational details on electronic structure as well as RRKM calculations are provided. The experimental results are presented in Sec. IV. Theoretical results are presented in Secs. V and VI. The discussion and conclusions are presented in Secs. VII and VIII.

II. EXPERIMENTAL SECTION

The scattering experiments were carried out using the improved CMB apparatus described in detail in Refs. 30 and 31. Briefly, two angle-collimated continuous supersonic beams of the reactants are crossed at 90° in the scattering chamber. During the experiments, the pressure is maintained in the 10^{-6} hPa range to ensure single collision conditions. The detector is a tunable electron impact ionizer followed by a quadrupole mass filter and an off-axis electron multiplier. The ionizer is located in the innermost region of a triply-differentially-pumped ultrahigh-vacuum chamber which is maintained in the 10^{-11} hPa pressure range in operating conditions by extensive turbo-pumping and liquid nitrogen cooling. The

detector unit can be rotated in the collision plane around the axis passing through the collision center. Reactant and product velocities are derived from time-of-flight (TOF) measurements.

Continuous supersonic beams of carbon atoms have been generated by the high-pressure radiofrequency (RF) discharge beam source successfully used in our laboratory to generate intense supersonic beams of transient species.[32,33] In this work, the supersonic beam of C atoms was produced by using 280 W of RF power on a dilute mixture of the molecular precursor CO(1.5%), in O_2(0.8%)/He (stagnation pressure of 60 mbar, nozzle diameter of 0.48 mm). In these conditions, atomic carbon is produced in the ground ^{3}P and excited ^{1}D electronic states in comparable amounts, as demonstrated by CMB studies of the C(^{1}D) + H_2/D_2 and C(^{3}P,^{1}D) + C_2H_2 reactions[5–8,13,14] and by measurements of electron-ionization efficiency curves of the carbon atom beam. The presence of C(^{3}P) does not represent a complication in the present experiments because the employed collision energy (E_c) is below the entrance barrier for the C(^{3}P) + CH_4 reaction.[4] The carbon beam peak velocity and speed ratio were 2344 m s^{-1} and 4.8, respectively. A supersonic beam of methane was produced by expanding a mixture of CH_4(25%) in He at a stagnation pressure of 1.9 bar through a stainless steel nozzle (0.1 mm diameter) kept at room temperature. Peak velocity and speed ratio were 1368 m s^{-1} and 11.6, respectively. The resulting collision energy was 25.3 kJ mol^{-1}. The nominal angular resolution of the detector for a point collision zone is 1°. The secondary target beam (CH_4 beam) was modulated at 160 Hz with a tuning fork chopper for background subtraction. Velocity distributions of the products were obtained at selected angles using the cross-correlation TOF technique with four 127-bit pseudorandom sequences. High-time resolution was achieved by spinning the TOF disk, located at the entrance of the detector, at 390.75 Hz corresponding to a dwell time of 5 μs/channel. Counting times varied from 60 to 360 min depending upon signal intensity.

The scattering measurements have been carried out in the laboratory (LAB) system of coordinates, while for the physical interpretation of the scattering process it is necessary to transform the data (angular, N(Θ), and time-of-flight, N(Θ, t) distributions) to a coordinate system which moves with the center-of-mass (CM) of the colliding system. Because of the finite resolution of the experimental conditions, i.e., finite angular and velocity spread of the reactant beams and angular resolution of the detector, the LAB-CM transformation is not single-valued and, therefore, analysis of the laboratory data is carried out by the usual forward convolution procedure. Trial CM angular and translational energy distributions are assumed, averaged, and transformed to the LAB frame for comparison with the experimental data until the best fit of the LAB distributions is achieved.

III. COMPUTATIONAL DETAILS AND RRKM CALCULATIONS

The potential energy surface of the system C(^{1}D) + CH_4 was investigated localizing the lowest stationary points at the B3LYP[34,35] level of theory in conjunction with the correlation consistent valence polarized set aug-cc-pVTZ.[36–38] At the same level of theory we compute the harmonic vibrational frequencies. The energy of all the stationary points was also computed at the higher level of calculation CCSD(T)[39–41] using the same basis set aug-cc-pVTZ. Both the B3LYP and the CCSD(T) energies were corrected to 0 K by adding the zero point energy correction computed as one-half the sum of the scaled harmonic vibrational frequencies evaluated at B3LYP/aug-cc-pVTZ level. The energy of C(^{1}D) was estimated by adding the experimental[2] separation C(^{3}P) – C(^{1}D) of 121.8 kJ mol^{-1} to the energy of C(^{3}P) at all levels of calculation. The energy of all the stationary points was computed also at the W1 (Refs. 42 and 43) level of theory. We remind that in the W1 method the geometry optimization and the evaluation of the frequencies are performed at the B3LYP/VTZ + *d* level while the energies are computed at the CCSD(T)/AVDZ + 2*d*, CCSD(T)/AVTZ + 2*d*1*f*, CCSD/AVQZ + 2*d*1*f* level of theory (AV*n*Z is for aug-cc-pV*n*Z with *n* = D, T, Q). All calculations were performed using GAUSSIAN 03[44] while the analysis of the vibrational frequencies was performed using MOLEKEL.[45]

We have performed RRKM calculations using the same code developed by us and described in previous papers.[24,46,47] The microcanonical rate constant for each elementary step is calculated using the formula

$$k(E) = N(E)/h\rho(E),$$

where N(E) denotes the sum of states in the transition state at energy E, ρ(E) is the reactant density of states at energy E and h is Planck's constant. N(E) is obtained by integrating the relevant density of states up to energy E and the rigid rotor/harmonic oscillator model is assumed. Both densities of states are appropriately symmetrized with respect to the number of identical configurations of the reactants and/or transition state. Where possible, tunneling and quantum reflection have been considered by using the corresponding imaginary frequency of the transition state and calculating the tunneling probability for the corresponding Eckart barrier.

In the cases where no transition state barrier has been identified in the electronic structure calculations (several dissociation steps), the corresponding microcanonical rate constants have been obtained in a variational way, evaluating k(E) at various points along the reaction coordinate and choosing the point which minimizes the rate constant. After all microcanonical rate constants have been calculated, a Markov (stochastic) matrix is set up for all intermediate and final channels in the reaction containing all branching ratios derived from the rate constants. This Markov matrix is subsequently raised to a high enough power to achieve convergence. In this way, the branching ratios for all product channels are calculated.

IV. RESULTS AND ANALYSIS OF REACTIVE SCATTERING EXPERIMENTS

The LAB angular distribution, N(Θ), at m/z = 26 ($C_2H_2^+$) was obtained by taking at least 5 scans of 50 s counting time at each angle. Attempts to measure LAB angular and TOF distributions at m/z = 27 ($C_2H_3^+$) failed, even when

trying the lowest practical ionizing electron energy in our ionizer (17 eV). That means that the products at $m/z = 27$ either do not live long enough to reach the detector (that is, they lose a secondary H atom in a time scale shorter than the detection timescale) or undergo complete dissociative ionization already at this low electron energy. The product angular and time-of-flight distributions recorded at $m/z = 26$, therefore, can correspond to the parent ion of C_2H_2 (produced in channel 2b) and H_2CC (produced in channel 2c), as well as to the daughter ion of vinyl radical (produced in channel 2a).

The main product of the H-displacement channels is expected to be the vinyl radical (channel 2a), because channel (2e) is much less competitive and, as we are going to see, the experimental energy release of the H-displacement channel is in line with the formation of vinyl + H. The ionization energy of vinyl radical is quite low (8.5 eV) and already at ~10 eV the energy is high enough to induce dissociative ionization. On the other hand, internally hot vinyl radical easily dissociates into C_2H_2 + H because of the relatively low energy barrier and exothermicity associated to the secondary H-loss; therefore, vinyl radicals formed with enough internal energy can dissociate before reaching the detector. In the photodissociation study of ethylene by Lee *et al.*,[20] in which the molecular co-fragments of H and H_2 have been detected by VUV photoionization, most C_2H_3 was found to further dissociate into C_2H_2 + H before reaching the detection zone (only 4% of the global amount of vinyl radicals was detected at $m/z = 27$ at a photon energy as low as 9.5 eV). Considering that Lee *et al.*[20] have used low energy photons (thus limiting dissociative ionization of vinyl radicals) and that the total available energy is roughly the same in the two experiments (762 kJ mol^{-1} taking as zero the energy level associated to ethylene, to be compared with 732 kJ mol^{-1} in the case of our experiment), we can infer that vinyl fragmentation is occurring in our experiment to a similar extent, which, accompanied by the possible dissociative ionization of the remaining C_2H_3 at the ionization energy employed in our experiment, prevents the measurements of the $m/z = 27$ distributions.

Since there was no advantage in working at a low energy of ionizing electrons, all the measurements presented here at $m/z = 26$ have been performed using an electron energy of 60 eV. The recorded LAB angular and TOF distributions are shown in Figures 1 and 2, respectively. In Figure 1 the error bars (representing ±1 standard deviation) are also shown. At small angles, the uncertainty associated to the recorded distributions was higher (and this is reflected in the larger error bars) because of the presence of an elastically scattered contamination from the primary beam (a small amount of CN radicals was present in the primary beam, probably because of a small air leak in the gas line. It is known, in fact, that in the presence of N_2, CN is also formed in the discharge[33,48]). This has made it necessary to subtract the elastic contribution at small angles, causing an increase of the error bars. Also the TOF spectra recorded at $\Theta = 20^\circ$ and 25° needed to be corrected for the elastic scattering signal and they appear noisier than the ones at larger angles (see Figure 2).

The LAB angular distribution (Figure 1) is quite wide, extending for about 60°, with a rounded peak located somewhat to the left of the center-of-mass position angle, Θ_{CM},

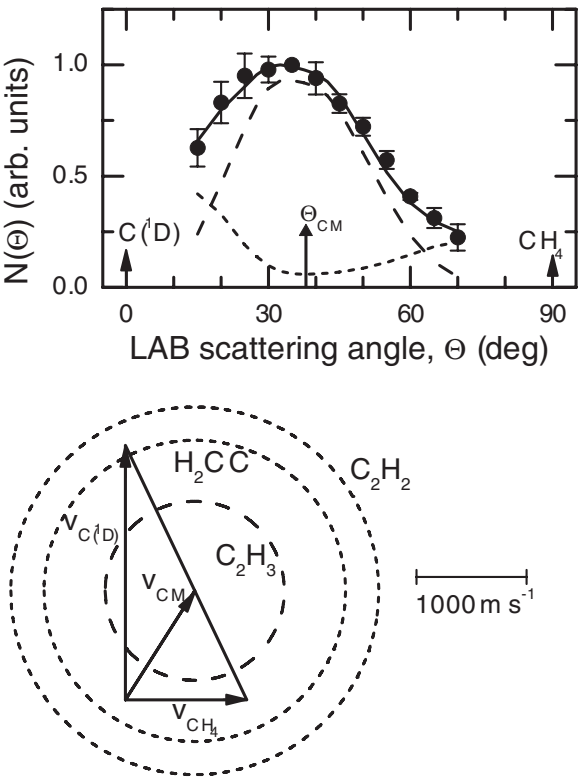

FIG. 1. Laboratory angular distribution, N(Θ), at $m/z = 26$ (solid circles) from the reaction $C(^1D) + CH_4$ at $E_c = 25.3$ kJ mol^{-1}, together with the velocity vector ("Newton") diagram of the experiment. Error bars represent ±1 standard deviation from the mean. The circles in the Newton diagram delimit the maximum speed that the indicated products can attain on the basis of linear momentum and energy conservation if all the available energy goes into product translational energy. The solid line is the total best-fit angular distribution. The separate contributions of the H-displacement and H_2-elimination channels C_2H_3 + H and C_2H_2/H_2CC + H_2 are indicated with dashed and short-dashed lines, respectively.

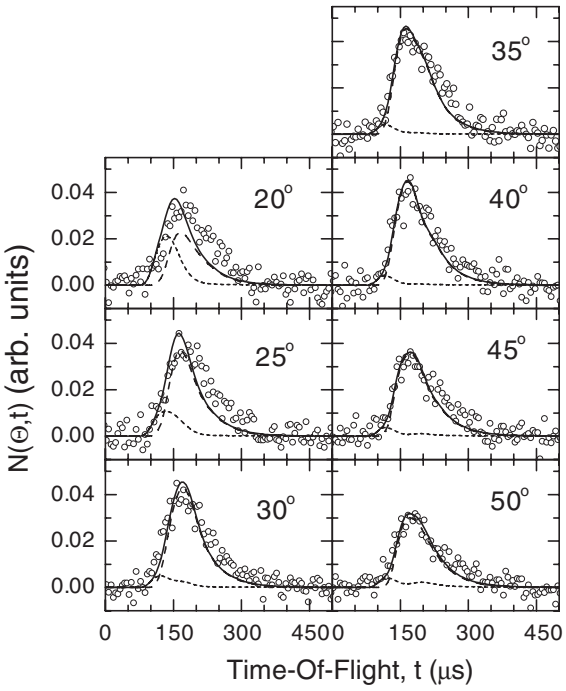

FIG. 2. Time-of-flight distributions recorded at $m/z = 26$ (open circles) for the reactions $C(^1D) + CH_4$ at $E_c = 25.3$ kJ mol^{-1} at the indicated LAB angles. Symbols are as in Figure 1.

indicating some preference for forward scattering. The TOF spectra are quite structureless and peak around the CM velocity (time).

The Newton diagram, displaying the system kinematics, is reported in the bottom panel of Figure 1. The overlapping Newton circles indicate the maximum center-of-mass speed that the heavy co-products of reaction channels 2a, 2b, and 2c can attain if all the available energy in each channel is converted into product translational energy. Those circles delimit the range of LAB angles within which each heavy co-product can be scattered. As is visible, the circles are quite different because of the different exothermicity and mass combination of the possible channels. In particular, the circle associated to channel 2a is significantly smaller than those associated to the H_2-elimination channels because of the reduced exothermicity and 27:1 mass combination. Therefore, the vinyl radical product is scattered into a smaller angular range with respect to either C_2H_2 or H_2CC. The circle corresponding to CCH_3 produced in channel 2e has not been reported in the diagram, but it is significantly smaller than that associated to C_2H_3 formed in channel 2a.

The fit of the $m/z = 26$ LAB angular and TOF distributions required the use of two components. One component (dashed lines in Figures 1 and 2) reproduces most features of the angular and TOF distributions. A second component (short-dashed lines in Figures 1 and 2), characterized by a much wider scattering range and fast TOF spectra, has been necessary to fit the wings of the LAB angular distribution, especially in the forward direction. Notably, also when considering the uncertainty associated to the intensity at small angles, the introduction of the second component remains necessary because there is some intensity missing also in the wing in the backward direction.

The two components into which the global distributions recorded at $m/z = 26$ have been separated during the best-fit procedure can be attributed to a contribution from the H-displacement channel (2a) and a contribution from one or both H_2-elimination channels (2b, 2c). As a matter of fact, the product energy release of the first contribution is compatible with the formation of vinyl radical +H, while the energy release for the second contribution is compatible with the channels $C_2H_2/H_2CC + H_2$. The best-fit CM distributions (with error bars) are reported in Figures 3 and 4 for the H-displacement and H_2-elimination channels, respectively. As far as the contribution associated to the H-displacement channel is concerned, we note that the best-fit CM angular distribution, $T(\theta)$, shows some intensity in the entire angular range with some propensity for forward scattering (as shown by the error bounds, the gray area in Figure 3, an isotropic angular distribution is only the upper limit of the range of functions giving an acceptable fit of the LAB distributions). For the best-fit $T(\theta)$, the ratio $T(180°)/T(0°)$ is 0.7, but this ratio can be reduced or extended from 0.6 and 1.0, as indicated by the error bound of Figure 3. The best-fit $T(\theta)$ is, therefore, consistent with the formation of a bound intermediate, the lifetime of which is comparable to its rotational period (osculating complex). The best-fit product translational energy distribution, $P(E'_T)$, is peaked around 35 kJ mol^{-1} and corresponds to an average product translational energy, $\langle E'_T \rangle$,

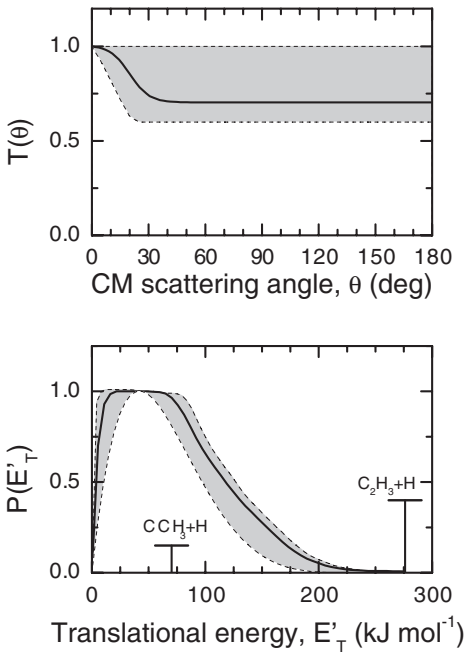

FIG. 3. Best fit CM product (top) angular and (bottom) translational energy distributions for the H-displacement channel.

of ~70 kJ mol^{-1}. The relative fraction of energy released as product translational energy, $\langle f'_T \rangle$, is ~0.25 if one considers the total energy associated to channel 2a. There is little sensitivity to the high energy cut-off of the $P(E'_T)$, but clearly the best-fit function is not compatible with the energetics of channel 2e. Finally, we can say that the fast rise of the best-fit $P(E'_T)$ seems to indicate that for this channel there is no exit barrier.

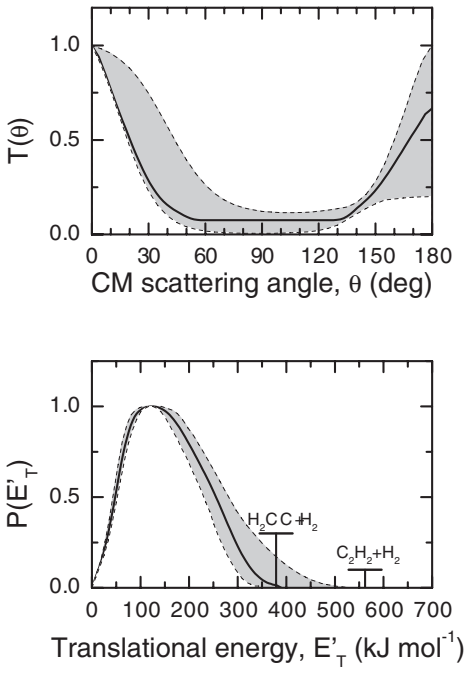

FIG. 4. Best fit CM product (top) angular and (bottom) translational energy distributions for the H_2-elimination channels.

The best-fit functions associated to the H_2-elimination channels (Figure 4) are quite different. The best-fit $T(\theta)$ is very polarized and it exhibits some preference for forward scattering. The best-fit $T(180°)/T(0°)$ is 0.67. A symmetric, strongly polarized $T(\theta)$ still produces an acceptable fit of the LAB distributions, while the lowest acceptable value of $T(180°)/T(0°)$ is 0.2. Also in the case of this channel, we can infer that the reaction mechanism is controlled by the presence of a bound intermediate with a lifetime comparable to its rotational period. The best-fit $P(E'_T)$ has a peak quite displaced from $E'_T = 0$ (at around 120 kJ mol^{-1}), suggesting that this channel is characterized by a sizeable exit barrier. The high energy cut-off does not furnish a clear-cut picture and we cannot distinguish between the formation of H_2CC or C_2H_2. Both channels 2b and 2c are compatible with the present determination. Notably, in both cases an exit barrier is present along the minimum energy paths (137 kJ mol^{-1} in the case of $HCCH_3$ dissociating into $C_2H_2 + H_2$ and 396 kJ mol^{-1} in the case of C_2H_4 dissociating into $H_2CC + H_2$). For this contribution, $\langle E'_T \rangle = 157$ kJ mol^{-1}, which corresponds to a fraction of energy released as product translational energy of ∼0.28 if one considers the total energy associated to channel 2b and ∼0.41 if one considers the total energy associated to channel 2c.

The determination of the branching ratio between the H-displacement and H_2-elimination channels is also affected by some uncertainty (we remind that in the case of a fit with multiple components, the relative yield is an adjustable parameter in the best-fit procedure). The best-fit ratio $\sigma(H_2)/\sigma(H)$ is 0.8, but it can vary by ±0.4.

V. COMPUTATIONAL RESULTS

The optimized structure of the main stationary points localized on the PES of $C(^1D) + CH_4$ are shown in Figure 5, while in Figure 6 we have reported a schematic representation of the PES. For the sake of simplicity, in Figure 6 only the relative energies computed at the more accurate W1 level are reported, while in Table I the values computed at all levels of calculation for comparison purposes are also shown. In Figure 5, we have reported also the optimized structure of $HCCH_3$ in its triplet ground state ($^3A''$), together with its relative energy with respect to C_2H_4 (^1A_g). The structures of the species shown in Figure 5 have been previously optimized by Chang *et al.* at the B3LYP/6-311G(d,p) level.[21,22] The agreement of our structures with those of Chang *et al.*[21,22] is very good, the differences being due to the different basis set employed in the present work. As expected, also the relative energies of the species shown in Figure 5 computed in the present work at the CCSD(T)/aug-cc-pVTZ//B3LYP/aug-cc-pVTZ level are in good agreement with those computed by Chang *et al.*[21,22] at the CCSD(T)/6-311+G(3df,3p)//B3LYP/6-311G(d,p) level. The structure of $HCCH_3$ in its triplet ground state has been previously computed by Kim *et al.*[4] at the QCISD/6-311G(d,p) level; our structure optimized at the B3LYP/aug-cc-pVTZ level is in good agreement with that computed by Kim *et al.*,[4] the main difference being the C–C bond distance (1.460 Å instead of 1.484 Å). However, the relative energy of $HCCH_3(^3A'')$ with respect to $C(^3P) + CH_4(^1A_1)$ computed in the present work at the CCSD(T)/aug-cc-pVTZ//B3LYP/aug-cc-pVTZ level (272.1 kJ mol^{-1}) is very close to the value computed by Kim *et al.*[4] at the CCSD(T)/6-311+G(3df,2p)//QCISD/6-311G(d,p) level (272.0 kJ mol^{-1}).

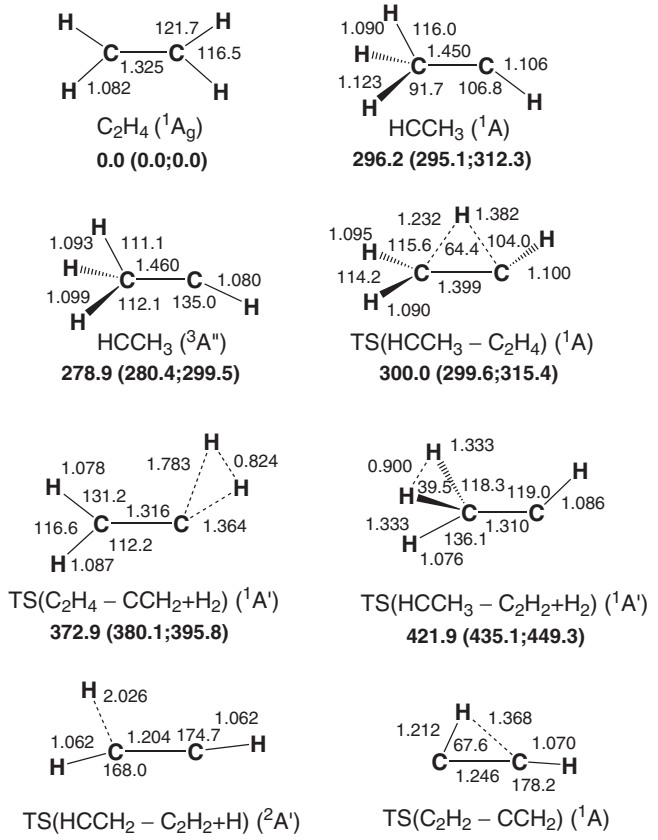

FIG. 5. B3LYP optimized geometries (Å and °) and relative energies (kJ mol^{-1}) at 0 K of minima and saddle points, localized on the PES of $C(^1D) + CH_4$; CCSD(T) and W1 relative energies are reported in parentheses. Also the saddle points for the reactions $HCCH_2 \rightarrow C_2H_2 + H$ and $C_2H_2 \rightarrow CCH_2$ are shown.

From Figure 6 we can see that, as expected, the favored approach for the reaction of $C(^1D)$ with CH_4 is the insertion of $C(^1D)$ into a C–H bond of CH_4. There is no barrier at least at the B3LYP level of calculation. Once formed, $HCCH_3$, in its excited singlet state, can isomerize to the global minimum C_2H_4 through a barrier of only 3.1 kJ mol^{-1} at the W1 level or can dissociate to $H + HCCH_2$ (channel 2a), $H + CCH_3$ (channel 2e) or $CH + CH_3$ (channel 2d). $HCCH_3$ can dissociate also to $C_2H_2 + H_2$ in an exothermic reaction which, however, is characterized by a significant barrier (137.0 kJ mol^{-1} at the W1 level). C_2H_4, in turn, can dissociate to $HCCH_2 + H$ or to $CCH_2 + H_2$; this latter reaction, however, shows a barrier as high as 395.8 kJ mol^{-1} at the W1 level. Also the structure of this transition state has been reported in Figure 5 together with the structure of the saddle connecting C_2H_2 with CCH_2, species which can be relevant for the reaction under investigation.

Finally, also the decomposition of C_2H_3 into $C_2H_2 + H$ has been characterized with the aim to understand whether the secondary H-loss is an efficient process for the vinyl radicals

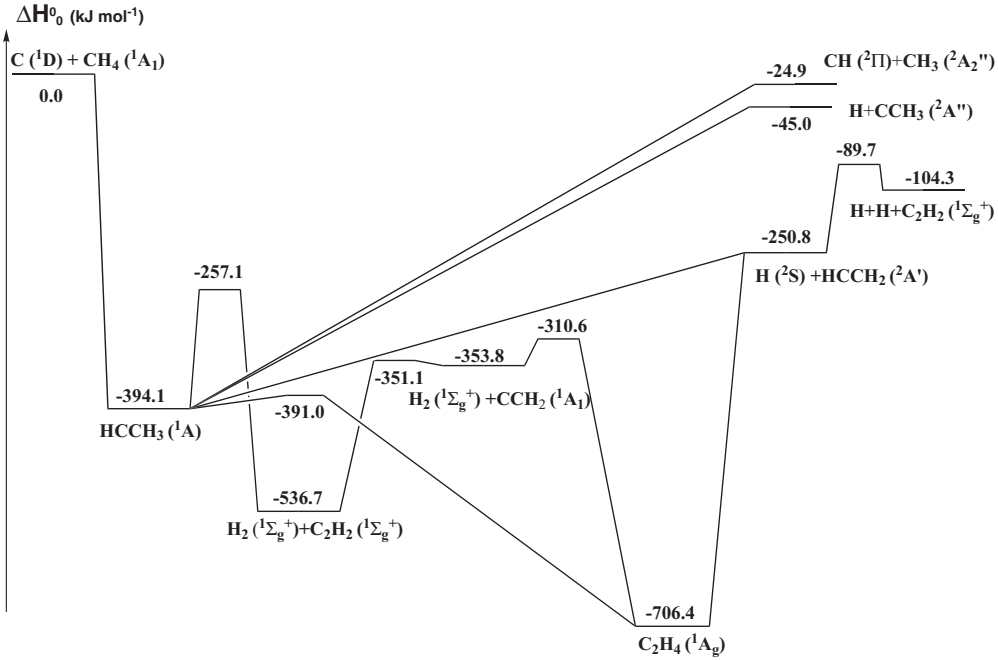

FIG. 6. Schematic representation of the $C(^1D) + CH_4$ potential energy surface. For simplicity, only the W1 relative energies (kJ mol^{-1}) are reported.

produced under the conditions of the present CMB experiment. The process is endothermic by 146.5 kJ mol^{-1} and a barrier of 161.1 kJ mol^{-1} needs to be surmounted.

VI. RRKM RESULTS

According to our calculations, the $HCCH_3$ intermediate formed by the insertion of $C(^1D)$ in a CH_4 bond can evolve in the following ways. (1) Elimination of an H atom from the methyl group to yield a vinyl radical, $HCCH_2$: this is the predominant channel with a rate constant of 1.12×10^{14} s^{-1} and a corresponding overall branching ratio of 0.952. The C–H bond which dissociates is one of the pre-existing bonds in methane. The dissociation of the newly formed C–H and C–C bonds is not competitive (see later). Notably, the lifetime of methylcarbene is very short (∼9 fs), shorter than the time scale (in the ps range) necessary for randomization of the available energy. In these conditions, RRKM basic assumptions are not warranted. (2) Rearrangement to yield an ethylene molecule, C_2H_4, with a rate constant of 7.78×10^{12} s^{-1}. This latter species can undergo further reactions (see below). Even though, on energetic grounds, rearrangement to form C_2H_4 would seem favored, the variational transition state for H loss to form a vinyl radical has an increased density of states due to the floppy motions of the outgoing H atom orthogonally to the reaction coordinate. This increased density of states strongly favors the formation of the vinyl radical. We remind that, since the H atom loss is treated variationally, any other possible transition state would yield an even higher rate constant. (3) Elimination of an H_2 molecule to yield an acetylene molecule, C_2H_2, with a rate constant of 1.35×10^{12} s^{-1}. The final branching ratio for the production of acetylene is 0.011, two orders of magnitude lower than the branching ratio of vinylidene (as are the rate constants). (4) Dissociation

TABLE I. Enthalpy changes and barrier heights (kJ mol^{-1}, 0 K) computed at the B3LYP/aug-cc-pVTZ, CCSD(T)/aug-cc-pVTZ, and W1 levels of theory for selected dissociation and isomerization processes for the system $C(^1D) + CH_4$.

	ΔH°_0			Barrier height		
	B3LYP	CCSD(T)	W1	B3LYP	CCSD(T)	W1
$C(^1D) + CH_4 \rightarrow HCCH_3$	− 393.3	− 379.2	− 394.1			
$HCCH_3 \rightarrow C_2H_4$	− 296.2	− 295.1	− 312.3	3.8	4.5	3.1
$HCCH_3 \rightarrow C_2H_2 + H_2$	− 134.2	− 134.1	− 142.6	125.7	140.0	137.0
$HCCH_3 \rightarrow CH + CH_3$	356.2	356.9	369.2			
$HCCH_3 \rightarrow CCH_3 + H$	339.2	345.6	349.1			
$HCCH_3 \rightarrow HCCH_2 + H$	139.9	146.8	143.3			
$C_2H_4 \rightarrow HCCH_2 + H$	436.1	441.9	455.6			
$C_2H_4 \rightarrow CCH_2 + H_2$	334.1	335.9	352.6	372.9	380.1	395.8
$HCCH_2 \rightarrow C_2H_2 + H$	160.2	146.8	146.5	168.7	162.9	161.1
$C_2H_2 \rightarrow CCH_2$	172.1	174.9	182.9	181.8	180.3	185.6

of one of the newly formed bonds to yield H + CCH_3 or CH + CH_3. Both of these channels are strongly endothermic and, as a result, their yield is minor (both rate constants are of the order of 10^7–10^8 s^{-1}, corresponding to branching ratios of the order of 10^{-6}).

Once formed, ethylene has the possibility of converting back to $HCCH_3$ and the rate constant for this process is 5.35 × 10^{11} s^{-1} (lower than the rate constant of the inverse reaction, since ethylene lies lower in energy than $HCCH_3$). Moreover, it can also lose an H atom to yield a vinyl radical, $HCCH_2$, with a rate constant of 1.4 × 10^{11} s^{-1}. The rate constant for hydrogen loss to a vinyl radical is around three orders of magnitude lower than the corresponding one of $HCCH_3$. This cannot be simply an effect of the reactant states (since the rate constants for interconversion between C_2H_4 and $HCCH_3$ do not differ by three orders of magnitude). We conclude, therefore, that in the case of ethylene the transition state for hydrogen atom loss hinders the reaction more than it does for $HCCH_3$.

Ethylene can also lose an H_2 molecule, yielding vinylidene (CCH_2), with a rate constant of 8.72 × 10^{11} s^{-1}. The overall branching ratio for vinylidene is 0.037. The branching ratio for vinylidene production is higher than that of acetylene, even though there is one more intermediate (ethylene) required for it. The reason for this lies in the higher rate constant (around one order of magnitude) for ethylene formation, coupled with the fact that this reaction is essentially irreversible. In any case, vinylidene and acetylene can interconvert to each other, with no possibility of any further rearrangement.

Finally, ethylene can dissociate into two $^3CH_2$ units. This reaction is strongly endothermic and its rate constant is extremely low (of the order of 10^5 s^{-1}). Thus, it is not considered here.

The resulting branching ratios determined at the E_c of the present experiment are summarized in Table II together with the rate constants. To be noted that the RRKM $\sigma(H_2)$ to $\sigma(H)$ ratio is at variance with the value derived from the analysis of the CMB results, even when considering the large uncertainty associated to the experimental determination.

A comparison with RRKM predictions for the photodissociation of C_2H_4 is in order, as it is quite well established that ethylene dissociation takes place on the ground C_2H_4 PES after fast interconversion of one of the excited states of ethylene populated by the absorption of UV photons. The total energy of our experiment amounts to 732 kJ mol^{-1}, to be compared with total energies of 619 kJ mol^{-1} (for the photodissociation at 193 nm) and 762 kJ mol^{-1} (for the photodissociation at 157 nm) considered by Chang *et al.*[21,22] For all the channels in common between reaction (2) and ethylene photodissociation, the present RRKM determination is quite in line with theirs, as our rate constants lie in between the values determined for ethylene photodissociation at the two energies. For instance, for rearrangement of C_2H_4 into $HCCH_3$, their rate constants are 3.21 × 10^{11} s^{-1} and 1.20 × 10^{12} s^{-1}, to be compared with our rate constant of 5.35 × 10^{11} s^{-1}. Similarly, for the H atom loss of C_2H_4 towards a vinyl radical, they obtain rate constants of 5.15 × 10^{10} s^{-1} and 9.27 × 10^{11} s^{-1}, to be compared with our 1.4 × 10^{11} s^{-1}. Finally, for the H_2 elimination, their rate constants are 1.09 × 10^{11} s^{-1} and 9.08 × 10^{11} s^{-1}, to be compared with our rate constant of 8.72 × 10^{11} s^{-1}.

Notably, as far as the $C_2H_4 \rightarrow HCCH_3$ rearrangement is concerned, despite the fact that our energy is closer to the higher energy of Chang *et al.*,[21,22] our rate constant is closer to the lowest of the two, indicating a convex increase of the rate constant (as would be expected from a rapid increase of the number of transition states available). The same is true for the H atom loss reaction, whereas the increase seems much more linear for the H_2 elimination reaction. In all cases, however, the order of importance of the three reactions is unambiguous. Quite interestingly, the rearrangement of ethylene into $HCCH_3$ is one of the dominant pathways in the ethylene dissociation.

Finally, in order to understand whether the primary vinyl product undergoes secondary H-loss in the timescale of the CMB experiment, we have calculated the rate constant for vinyl dissociation into C_2H_2 + H. Assuming an average recoil energy for the departing primary H atom of 70 kJ mol^{-1} (as indicated by the determination of the product energy release) the vinyl radical $HCCH_2$ decays into an acetylene molecule HCCH and another H atom with a rate constant of around 7.86 × 10^7 s^{-1}, which implies an approximate lifetime of around 13 ns for the vinyl radical. We note that tunneling makes a significant contribution to this process, both due to the fact that the internal energy of the vinyl radical is near the barrier and that the reaction coordinate involves the motion of a light atom. Such a short lifetime implies that the vinyl radicals produced in channel 2a under the conditions of the present CMB experiment could never be detected at $m/z = 27$ (the time scale of the experiment is of a few hundreds of microseconds).

TABLE II. Rate constants (k, in s^{-1}) and branching ratios (BR,%) for the reaction $C(^1D) + CH_4$ at $E_c = 25.3$ kJ mol^{-1}.

	k	BR
$HCCH_3 \rightarrow C_2H_4$	7.78 × 10^{12}	
$HCCH_3 \rightarrow C_2H_2 + H_2$	1.35 × 10^{12}	1.1
$HCCH_3 \rightarrow CH + CH_3$	2.53 × 10^8	
$HCCH_3 \rightarrow CCH_3 + H$	2.0 × 10^9	
$HCCH_3 \rightarrow HCCH_2 + H$	1.12 × 10^{14}	95.2
$C_2H_4 \rightarrow HCCH_3$	5.35 × 10^{11}	
$C_2H_4 \rightarrow HCCH_2 + H$	1.4 × 10^{11}	
$C_2H_4 \rightarrow CCH_2 + H_2$	8.72 × 10^{11}	3.7
$C_2H_4 \rightarrow CH_2 + CH_2$	3.50 × 10^5	
$HCCH_2 \rightarrow C_2H_2 + H$	7.86 × 10^7	

VII. DISCUSSION

One important issue arising from the comparison between the present experimental findings and the RRKM treatment is whether the insertion intermediate is so short-lived as indicated by RRKM calculations or if it lives at least for a few rotational periods, as suggested by the best-fit $T(\theta)$ derived for the contribution associated to the H-displacement channel. It is difficult to reconcile these opposite findings: typically, the deviations from a statistical behavior caused by dynamical

effects manifest themselves when the intermediate lifetime is short. On the contrary, in this case the dynamical observables pointed to a relatively long-lived complex (osculating), while RRKM calculations derived a lifetime of a few femtoseconds. RRKM basic assumptions lose their validity with such a short lifetime because energy redistribution, as well as isomerization to the much more stable ethylene intermediate, require that methylcarbene has a long enough lifetime. Under these circumstances, only dynamical calculations on accurate multidimensional PES can clarify the reaction mechanism.

At this stage, we can only put forward some suggestions. A possible explanation for the increase of methylcarbene lifetime is associated to the coupling with the triplet PES supporting methylcarbene in its ground state. The two states are quite close in energy and Kim *et al.*[4] in their theoretical investigation of reaction (1) have identified a seam of crossing between the triplet and the singlet state in the vicinity of the methylcarbene configuration. Remarkably, the singlet-triplet energy difference is much smaller in the case of methylcarbene than in the case of carbene, for which, as already mentioned in the Introduction, there is some evidence that the two states are strongly mixed. If fast ISC from the singlet to the triplet PES takes place during the $HCCH_3$ formation, then it would be easy to rationalize our experimental observation of a CM best-fit function with some intensity in the entire angular range (see Figure 3). Kim *et al.*[4] have derived an RRKM rate constant for triplet methylcarbene dissociating into vinyl + H of 9.75×10^{12} s^{-1} at an energy of 193 kJ mol^{-1} above the $C(^3P) + CH_4$ asymptote (the corresponding quantity in our experiment would be 147.1 kJ mol^{-1}). Therefore, if a jump from the singlet to the lower triplet state PES occurs, the intermediate lifetime becomes significantly longer. This is not the only possible explanation. In this case, as well as in that of the related $C(^1D) + H_2$ reaction, the fivefold degeneracy of $C(^1D)$ is lifted by its interaction with methane and more than one PES could contribute to the global outcome recorded in our experiment. A significant contribution from an excited state PES supporting a long-lived intermediate complex could explain our findings. In this respect, it should be noted that a fast conversion of excited states to the ground state of ethylene has been found to occur via non-adiabatic pathways in the photodissociation and photoisomerization of ethylene.[21,22,49]

In conclusion, this system, which is relatively simple involving only six atoms of which four are H atoms, could become a benchmark to study nonadiabatic effects of various kinds. We would like to note that quasiclassical trajectory calculations on multidimensional PESs have become available in recent years for systems of similar complexity, such as $O(^3P) + C_2H_2$ (Ref. 50) and C_2H_4.[51–53]

Some interesting indications also come from the comparison of our experimental findings with those obtained for the VUV photodissociation of ethylene, which has been widely investigated over many years (see Refs. 19 and 20, and references therein). There is general agreement on the fact that the electronically excited states of ethylene populated after the absorption of UV photons at 193 and 157 nm are connected to the ground state via conical intersections and that the photodissociation of ethylene can be described as occurring on the ground state C_2H_4 PES. As already commented on, the electronic structure and RRKM calculations are very similar for reaction (2) and ethylene photodissociation, the most importance difference being the RRKM-predicted fast dissociation of methylcarbene into vinyl +H (this process was not considered by Chang *et al.*,[21,22] as already pointed out by Lee *et al.*[20] to explain the disagreement between experimental and RRKM branching ratios for the photodissocation of ethylene and its deuterated isotopomers). If we compare the experimental results, they are impressively similar. For instance, the $m/z = 26$ signal recorded in the experiment at 157 nm has been attributed to the H_2-elimination channel for 46% and to the H-elimination channel for 54%.[20] The resulting $\sigma(H_2)/\sigma(H)$ is 0.88, which nicely compares with our determination of 0.8 ± 0.4. In addition, the product translational energy distribution derived for the H atoms[19] has a peak at 34 kJ mol^{-1} and corresponds to an $\langle E'_T \rangle$ of 52 kJ mol^{-1}, to be compared with our values of 35 kJ mol^{-1} and 70 kJ mol^{-1}: the agreement is excellent if one considers that in the determination of the H energy release, primary and secondary H atoms could not be distinguished.[19] Furthermore, the product translational energy distribution derived for H_2 products has a peak at 126 kJ mol^{-1} and corresponds to $\langle E'_T \rangle$ of 166 kJ mol^{-1}, to be compared with our values of 120 kJ mol^{-1} and 157 kJ mol^{-1}. Clearly, the two processes are experiencing the same PES regions, especially in the case of the H_2 elimination channel. The similarity between the two sets of results would be very easy to explain if reaction (2) were dominated by the formation of ethylene via isomerization of methylcarbene, in contrast with what suggested by the present RRKM prediction.

It is also interesting to compare the results of the present study with similar ones on the related systems $O(^1D) + CH_4$, $N(^2D) + CH_4$ and $S(^1D) + CH_4$, which have been already investigated in CMB experiments. In all cases, the first step is insertion of the atomic species in its electronically excited state into one of the C–H bonds. The formed insertion intermediates (CH_3OH, CH_3NH, CH_3SH) all reside in deep potential wells, deeper than that associated to methylcarbene, the insertion intermediate of reaction (2). In terms of the reaction mechanism, perhaps the most similar system is $N(^2D) + CH_4$: in that case as well, the favored channel is the one leading to $CH_2NH + H$, that is, one of the pre-existing C–H bonds breaks apart, rather than the newly formed N–H or C–H bonds.[24] There is some competition by the new N–H and C–H bond breaking channels with the increase of the available energy, because the intermediate lifetime shortens with the total energy and the energy excess initially concentrated in the two newly formed bonds does not have time to redistribute.[24] Surprisingly, notwithstanding the predicted short lifetime of the insertion intermediate, this is not the case for reaction (2), because we did not get any evidence of channel 2e (incidentally, we would like to note that the CM-LAB transformation Jacobian would greatly enhance its presence in our LAB distributions). The H_2-elimination channel was not open in the case of the $N(^2D) + CH_4$ reaction.

The results on reaction (2) are difficult to compare with those on $S(^1D) + CH_4$ because, in that case, the only open channel is the C–S bond breaking channel with the

formation of SH + CH_3 (all the other channels are either endothermic or characterized by a high exit barrier).[25] Nevertheless, the two systems have in common the pronounced polarization of the best-fit T(θ) observed for the channels SH + CH_3 and $H_2CC/C_2H_2 + H_2$. Quite interestingly, if we analyze the structures of the transition states associated to $HCCH_3 \rightarrow C_2H_2 + H_2$ and $C_2H_4 \rightarrow H_2CC + H_2$, the one associated to the three-center elimination of H_2 from ethylene is lying on a plane and, as such, perfectly matches with the observation of a polarized best-fit T(θ). This might be taken as an indication that H_2CC is predominantly formed under the conditions of our CMB experiment.

As in the S(^{1}D) + CH_4 reaction, also in O(^{1}D) + CH_4 it is the newly (C–O) bond formed in the insertion process that breaks apart preferentially leading to the strongly exoergic ($\Delta H^\circ_0 \sim -180$ kJ mol^{-1}) CH_3 + OH product channel.[23] In the C(^{1}D) + CH_4 reaction the corresponding pathway is that leading to CH + CH_3, but this is much less exoergic in this system (the least exoergic of all, with $\Delta H^\circ_0 = -24.9$ kJ mol^{-1}—see Figure 6) and is not observed in the present experiment, neither is predicted statistically to be relevant. The main channel in the C(^{1}D) reaction is the strongly exoergic ($\Delta H^\circ_0 = -250.8$ kJ mol^{-1}) H + CH_2CH forming channel, whose analogue in the O(^{1}D) reaction is the H + CH_2OH (CH_3O) channel which has $\Delta H^\circ_0 = -152$ (116) kJ mol^{-1} and a lower (18%) yield. Notably, in the O(^{1}D) reaction the H_2 channel accounts for only 5% of the yield, with comparable amounts of H_2CO ($\Delta H^\circ_0 = -473$ kJ mol^{-1}) and HCOH ($\Delta H^\circ_0 = -268$ kJ mol^{-1}) being formed, while in the C(^{1}D) reaction the corresponding pathways $H_2CC + H_2$ ($\Delta H^\circ_0 = -353{,}8$ kJ mol^{-1}) and HCCH + H_2 ($\Delta H^\circ_0 = -536.7$ kJ mol^{-1}) are comparatively much more important (45%), and this is likely due to the quite different topology of the PES for O(^{1}D) + CH_4 in which there is no intermediate equivalent to the very stable C_2H_4 molecule. Interestingly, the T(θ) for the H_2 channel is strongly polarized for C(^{1}D) while in the O(^{1}D) reaction is isotropic. This can be rationalized in terms of the different geometry of the decomposing transition state which is planar (from C_2H_4) in the case of the C(^{1}D) reaction, as discussed above.

VIII. CONCLUSIONS

The mechanism of reaction (2) has been investigated by CMB experiments and electronic structure calculations of the underlying PES. RRKM estimates of the product branching ratios have been performed using the *ab initio* PES. The experimental results can be explained by considering the competition between H-displacement and H_2-elimination channels. The two mechanisms appear to be of equal importance, with a best estimate of $\sigma(H_2)/\sigma(H) = 0.8$. For both channels, the reaction mechanism is controlled by the presence of a bound intermediate, the lifetime of which is comparable to its rotational period. The pronounced polarization of the best-fit CM angular distribution associated to the H_2-elimination channel indicates that the formation of vinylidene should be more important than the formation of acetylene. On the contrary, RRKM estimates predict a very short lifetime for the insertion intermediate (so short that RRKM assumptions themselves are not warranted) and the dominance of the H-displacement channel. A first conclusion is that reaction (2) cannot be described statistically and RRKM branching ratios cannot be used as such in the interpretation of the experiment. A dynamical treatment is necessary to understand its reaction mechanism. Possibly, nonadiabatic effects are responsible for the discrepancies, as triplet and singlet PES of methylcarbene cross each other and ISC is possible.

The strong similarities with the experimental results on the photodissociation of ethylene point to the fact that the two systems experience the same regions of the PES, so indirectly confirming that ethylene photodissociation can be described as occurring on the ground state C_2H_4 PES.

A comparison with the analogous reactions O(^{1}D) + CH_4, N(^{2}D) + CH_4 and S(^{1}D) + CH_4 indicates similarities and differences. These systems are promising new benchmarks for the theoretical treatment of more complex insertion reactions after the role played by the much simpler O(^{1}D) + H_2,[54,55] N(^{2}D) + H_2,[56,57] S(^{1}D) + H_2,[58,59] and C(^{1}D) + H_2.[5–8] We remind that the mechanism of insertion reactions is extremely interesting in many fields, since insertive reactions are involved in a variety of natural and applied phenomena.

ACKNOWLEDGMENTS

We acknowledge financial support from the Italian MIUR (Ministero Istruzione Università Ricerca) under project PRIN 2009SLKFEX_004 and COST Action CM0805 The Chemical Cosmos: Understanding Chemistry in Astronomical Environments. R. Petrucci thanks FSE (Fondo Sociale Europeo) – Regione Umbria – Ministero del Lavoro e delle Politiche Sociali for a fellowship. We thank A. Bergeat and G. Capozza for their contribution in the early stages of the experimental part of this work.

[1] K. Schofield, J. Phys. Chem. Ref. Data **8**, 723 (1979).
[2] C. E. Moore, "Atomic energy levels," Natl. Bur. Stand. (U.S.) Circ. No. 467 (U.S. Government Printing Office, Washington, DC, 1949).
[3] L. B. Harding, R. Guadagnini, and G. C. Schatz, J. Phys. Chem. **97**, 5472 (1993).
[4] G.-S. Kim, T. L. Nguyen, A. M. Mebel, S. H. Lin, and M. T. Nguyen, J. Phys. Chem. A **107**, 1788 (2003).
[5] A. Bergeat, L. Cartechini, N. Balucani, G. Capozza, L. F. Phillips, P. Casavecchia, G. G. Volpi, L. Bonnet, and J.-C. Rayez, Chem. Phys. Lett. **327**, 197 (2000).
[6] N. Balucani, G. Capozza, L. Cartechini, A. Bergeat, R. Bobbenkamp, P. Casavecchia, F. J. Aoiz, L. Bañares, P. Honvault, B. Bussery-Honvault, and J.-M. Launay, Phys. Chem. Chem. Phys. **6**, 4957 (2004).
[7] N. Balucani, G. Capozza, E. Segoloni, A. Russo, R. Bobbenkamp, P. Casavecchia, T. Gonzalez-Lezana, E. J. Rackham, L. Bañares, and F. J. Aoiz, J. Chem. Phys. **122**, 234309 (2005).
[8] N. Balucani, P. Casavecchia, F. J. Aoiz, L. Bañares, J.-M. Launay, B. Bussery-Honvault, and P. Honvault, Mol. Phys. **108**, 373 (2010).
[9] P. Defazio, B. Bussery-Honvault, P. Honvault, and C. Petrongolo, J. Chem. Phys. **135**, 114308 (2011).
[10] R. Guadagnini and G. C. Schatz, J. Phys. Chem. **100**, 18944 (1996).
[11] R. Van Harrevelt, M. C. Van Hemert, and G. C. Schatz, J. Chem. Phys. **116**, 6002 (2002).
[12] R. I. Kaiser, A. M. Mebel, and Y. T. Lee, J. Chem. Phys. **114**, 231 (2001).
[13] F. Leonori, R. Petrucci, E. Segoloni, A. Bergeat, K. M. Hickson, N. Balucani, and P. Casavecchia, J. Phys. Chem. A **112**, 1363 (2008).
[14] M. Costes, N. Daugey, C. Naulin, A. Bergeat, F. Leonori, E. Segoloni, R. Petrucci, N. Balucani, and P. Casavecchia, Faraday Discuss. **133**, 157 (2006).

[15]R. I. Kaiser, T. L. Nguyen, A. M. Mebel, and Y. T. Lee, J. Chem. Phys. **116**, 1318 (2002).
[16]D. C. Scott, J. de Jaun, C. C. Robie, D. Schwartz-Lavi, and H. Reisler, J. Phys. Chem. **96**, 2509 (1992).
[17]M. R. Scholefield, J.-H. Choi, S. Goyal, and H. Reisler, Chem. Phys. Lett. **288**, 487 (1998).
[18]G. E. Hall, A. V. Komissarov, and T. J. Sears, J. Phys. Chem. A **108**, 7922 (2004).
[19]J. J. Lin, C. C. Wang, Y. T. Lee, and X. Yang, J. Chem. Phys. **113**, 9668 (2000).
[20]S.-H. Lee, Y. T. Lee, and X. Yang, J. Chem. Phys. **120**, 10983 (2004).
[21]A. H. H. Chang, A. M. Mebel, X. Yang, S. H. Lin, and Y. T. Lee, Chem. Phys. Lett. **287**, 301 (1998).
[22]A. H. H. Chang, A. M. Mebel, X. Yang, S. H. Lin, and Y. T. Lee, J. Chem. Phys. **109**, 2748 (1998).
[23]J. J. Lin, J. Shu, Y. T. Lee, and X. Yang, J. Chem. Phys. **113**, 5287 (2000).
[24]N. Balucani, A. Bergeat, L. Cartechini, G. G. Volpi, P. Casavecchia, D. Skouteris, and M. Rosi, J. Phys. Chem. A **113**, 11138 (2009).
[25]C. Berteloite, S. D. Le Picard, I. R. Sims, M. Rosi, F. Leonori, R. Petrucci, N. Balucani, X. Wang, and P. Casavecchia, Phys. Chem. Chem. Phys. **13**, 8485 (2011).
[26]P. P. Saxena, P. S. Bhatnagar, and M. Singh, Mon. Not. R. Astron. Soc. **334**, 563 (2002).
[27]K. Magee-Sauer, M. J. Mumma, M. A. DiSanti, N. Dello Russo, E. L. Gibb, B. P. Bonev, and G. L. Villanueva, Icarus **194**, 347 (2008), and references therein.
[28]G. P. Tozzi, P. D. Feldman, and M. C. Festou, Astron. Astrophys. **330**, 753 (1998).
[29]J. Luque, W. Juchmann, E. A. Brinkman, and J. B. Jeffries, J. Vac. Sci. Technol. A **16**, 397 (1998).
[30]N. Balucani, G. Capozza, F. Leonori, E. Segoloni, and P. Casavecchia, Int. Rev. Phys. Chem. **25**, 109 (2006).
[31]P. Casavecchia, F. Leonori, N. Balucani, R. Petrucci, G. Capozza, and E. Segoloni, Phys. Chem. Chem. Phys. **11**, 46 (2009).
[32]M. Alagia, V. Aquilanti, D. Ascenzi, N. Balucani, D. Cappelletti, L. Cartechini, P. Casavecchia, F. Pirani, G. Sanchini, and G. G. Volpi, Isr. J. Chem. **37**, 329 (1997).
[33]F. Leonori, K. M. Hickson, S. D. Le Picard, X. Wang, R. Petrucci, P. Foggi, N. Balucani, and P. Casavecchia, Mol. Phys. **108**, 1097 (2010).
[34]A. D. Becke, J. Chem. Phys. **98**, 5648 (1993).
[35]P. J. Stephens, F. J. Devlin, C. F. Chabalowski, and M. J. Frisch, J. Phys. Chem. **98**, 11623 (1994).
[36]T. H. Dunning, Jr., J. Chem. Phys. **90**, 1007 (1989).
[37]D. E. Woon and T. H. Dunning, Jr., J. Chem. Phys. **98**, 1358 (1993).
[38]R. A. Kendall, T. H. Dunning, Jr., and R. J. Harrison, J. Chem. Phys. **96**, 6796 (1992).
[39]R. J. Bartlett, Annu. Rev. Phys. Chem. **32**, 359 (1981).
[40]K. Raghavachari, G. W. Trucks, J. A. Pople, and M. Head-Gordon, Chem. Phys. Lett. **157**, 479 (1989).
[41]J. Olsen, P. Jorgensen, H. Koch, A. Balkova, and R. J. Bartlett, J. Chem. Phys. **104**, 8007 (1996).
[42]J. M. L. Martin and G. de Oliveira, J. Chem. Phys. **111**, 1843 (1999).
[43]S. Parthiban and J. M. L. Martin, J. Chem. Phys. **114**, 6014 (2001).
[44]M. J. Frisch, G. W. Trucks, H. B. Schlegel *et al.*, GAUSSIAN 03, Revision D.01, Gaussian, Inc., Wallingford, CT, 2004.
[45]MOLEKEL 4.3, P. Flükiger, H. P. Lüthi, S. Portmann, and J. Weber, Swiss Center for Scientific Computing, Manno (Switzerland), 2000–2002.
[46]F. Leonori, R. Petrucci, N. Balucani, P. Casavecchia, M. Rosi, D. Skouteris, C. Berteloite, S. D. Le Picard, A. Canosa, and I. R. Sims, J. Phys. Chem. A **113**, 15328 (2009).
[47]N. Balucani, F. Leonori, R. Petrucci, M. Stazi, D. Skouteris, M. Rosi, and P. Casavecchia, Faraday Discuss. **147**, 189 (2010).
[48]F. Leonori, R. Petrucci, X. Wang, P. Casavecchia, and N. Balucani, Chem. Phys. Lett. **553**, 1 (2012).
[49]M. Ben-Nun and T. J. Martinez, Chem. Phys. Lett. **298**, 57 (1998).
[50]K. Rajak and B. Maiti, J. Chem. Phys. **133**, 011101 (2010).
[51]W. Hu, G. Lendvay, B. Maiti, and G. C. Schatz, J. Phys. Chem. A **112**, 2093 (2008).
[52]B. Fu, Y.-C. Han, J. M. Bowman, L. Angelucci, N. Balucani, F. Leonori, and P. Casavecchia, Proc. Natl. Acad. Sci. U.S.A. **109**, 9733 (2012).
[53]B. Fu, Y.-C. Han, J. M. Bowman, F. Leonori, L. Angelucci, N. Balucani, A. Occhiogrosso, R. Petrucci, and P. Casavecchia, J. Chem. Phys. **137**, 22A532 (2012).
[54]N. Balucani, P. Casavecchia, F. J. Aoiz, L. Bañares, J. F. Castillo, and V. J. Herrero, Mol. Phys. **103**, 1703 (2005).
[55]F. J. Aoiz, L. Banares, J. F. Castillo, V. J. Herrero, B. Martinez-Haya, P. Honvault, J.-M. Launay, X. Liu, J. J. Lin, S. A. Harich, C. C. Wang, and X. Yang, J. Chem. Phys. **116**, 10692 (2002).
[56]N. Balucani, L. Cartechini, G. Capozza, E. Segoloni, P. Casavecchia, G. G. Volpi, F. J. Aoiz, L. Bañares, P. Honvault, and J.-M. Launay, Phys. Rev. Lett. **89**, 013201 (2002).
[57]N. Balucani, P. Casavecchia, L. Bañares, F. J. Aoiz, T. Gonzalez-Lezana, P. Honvault, and J.-M. Launay, J. Phys. Chem. A **110**, 817 (2006).
[58]S. H. Lee and K. Liu, J. Phys. Chem. A **102**, 8637 (1998).
[59]C. Berteloite, M. Lara, A. Bergeat, S. D. Le Picard, F. Dayou, K. M. Hickson, A. Canosa, C. Naulin, J.-M. Launay, I. R. Sims, and M. Costes, Phys. Rev. Lett. **105**, 203201 (2010).